

Dynamics and Thermodynamics of Dense and Dilute Clusters of Drops

J. Bellan

Jet Propulsion Laboratory
4800 Oak Grove Drive
Pasadena, Ca. 91109
U.S.A.

1 Introduction

Collective drop behavior is encountered in sprays produced for a variety of applications : fuel sprays produced for combusting devices, metal sprays produced for coating, paint sprays, printer sprays, atmospheric clouds, etc.. There is experimental evidence that clusters of drops exist both in combusting [1], [2], [3], [4], [5], and non-combusting sprays for atomizers used in combusting devices [6], [3], [4] . Clusters of drops have also been observed in round jets laden with solid glass beads [7], although the glass beads (of 55 μ radius) did not behave entirely like liquid drops due to their large inertia. The existence of these clusters of drops indicates that the interaction among the drops is important in determining the dynamics of the drops because the drop proximity changes the flow around the individual drops in ways that affects the drag on each drop. Additionally, if there is a phase change between the liquid drops and the gaseous surroundings (either evaporation or condensation), this will also influence the flow around the individual drops ; and phase change is also affected by the drop proximity. If evaporation occurs, it is the drop heat up that is affected by drop proximity and the build up of fuel vapor in the interstitial space among drops might lead to saturation of the gas, resulting in termination of evaporation. If condensation occurs, such as in atmospheric clouds, the rate of mass transfer to the hotter liquid drops from the colder gas results in the reduction of the temperature differential between phases and thus might terminate phase change ; and the rate of mass transfer depends upon drop proximity.

These **simple** examples illustrate the difficulty of studying the dynamics of clusters of drops in all flows : the intimate coupling between the dynamics and the thermodynamics of the drops with the flow around the drops, and the nonlinearities involved in this coupling present a formidable challenge both to the experimentalists and to the modelers. Moreover, most flows encountered in practical situations are turbulent, thus compounding the difficulties.

The point of departure for the understanding of the complex interactions among drops and flow is the behavior of a single, isolated particle in a turbulent flow ; such studies have been carried out either with individual drops or with dilute collections of drops where the very large distance between particles compared to the size of the particles made them behave as if they were isolated from each other. Although there have been many interesting studies of isolated drop behavior, both experimentally and theoretically, such as [8] , [9] , [10], [11], [12], it is the body of studies performed by Crowe and his coworkers [13], [14], [15] which has provided a systematic frame for categorizing the interactions between drops and flow in the context of sprays through the Stokes number, $St = 2\rho_l R^2 \Delta u / (9\mu_g L)$, where ρ_l is the liquid density, R is the drop radius, Δu is a characteristic velocity slip between drops and gas, μ_g is the gas viscosity, and L is a characteristic length associated with the gas flow. The Stokes number had been previously used to study the interaction between a particle and a flow, but in the context of a spray it is interpreted to quantify the interaction between turbulent structures of various scales and the drops.- Figure 1 reproduced from [14] shows the fate of the drops according to their Stokes-number. Thus, if $St \ll 1$, the drops follow faithfully the flow; if $St \gg 1$, the drops do not have time to interact with the flow **and** their behavior is then independent of the flow ; and if $St = 0(1)$, then the drops interact with the flow and there is a slip velocity between drops and flow. Further experimental work by Goix and Edwards[16] confirmed this discrimination of the drops motion in terms of the Stokes number. It should be noticed that in order to calculate the Stokes number, one has to be able to calculate accurately this slip velocity.

For a single drop, the calculation of the slip velocity involves well-established equations [11] . In particular, the definition of the drag force on a drop implies that the velocity field around a drop is accurately known. Thus, the conventional formalism can be used only when one *can* measure or calculate the velocity field at a scale smaller than the drop spacing.

In most realistic situations, it is impossible and/or practical to know the velocity between the drops, especially in dense regions of a spray. This is because the scale of the spray is several orders of magnitude larger than the scale of the interdrop distance, and practical information is always sought at the scale of the spray. Thus, other strategies must be used to calculate the dynamics of the collections of drops in a flow.

The strategy proposed here is to categorize the multitude of scales in a spray into two classes : the macroscale and the microscale. The macroscale is the scale

associated with the scale of the spray, whereas the **microscale** is that associated with the interdrop interaction. It is proposed that in a first step each scale be studied uncoupled from the other and that ultimately they be coupled in a model that will encompass the entire spray. One of the earliest attempts to consider the effect of the **microscale** upon the **macroscale** has been made by Chiu and his coworkers [17], [18], who introduced a characteristic number to qualify the drop interaction, however the evaporation rate used in its calculation was that of the single, isolated drop and so the calculation gave a qualitative estimate rather than a quantitative result. Modeling of the **microscale** in terms of collections of drops has been performed by Bellan and Cuffel [19], Bellan and Harstad [20], [21], [22], by Harstad and Bellan [23], [24], and by Yang and Sichel [25]. In the models of Yang and Sichel, evaporation of the drops is calculated only in the dilute regime, the assumption having been made that in the dense regime the interstitial gas is saturated. Thus the thermodynamics and the dynamics of the drops are uncoupled

What will be described in the following are studies of collections of drops where the dynamics and thermodynamics of the drops are coupled. This means that the modification of the drag force due to the drop number density, the evaporation rate and the slip velocity are all taken into account. In turn, the enhancement in the evaporation rate due to the slip velocity, and the hindering of evaporation due to the drop proximity are also part of the models.

2 Clusters of Monodisperse Single-component Drops in Axial Flows

It has often been argued that from the thermodynamic point of view, a cluster of drops behaves in fact as one large drop of the same dimension as the cluster, having an evaporation rate which is the sum of the evaporation rates of all drops at the periphery of the cluster. Models uncoupling the dynamics and the thermodynamics of interacting drops, such as [25], support this assumption. Their results show that clusters of drops burn with an external flame sustained by fuel vapor supplied by the drops located at the cluster boundary. This vaporization sheet propagates inward from the boundary of the cluster as the cluster shrinks, the outermost drops disappearing before the immediately adjacent drops start evaporating.

2.1 General Results

The physical picture of the cluster of drops as an equivalent large drop is not supported by results obtained with models coupling dynamics and thermodynamics of interacting drops, such as [26]. In this model, the evaporation rate is calculated using the concept of the "sphere of influence" [19]. By definition, each drop is surrounded by a fictitious sphere of influence centered at the drop's center and having for radius

the half distance between the centers of two adjacent drops. Thus, the cluster volume is the volume of all spheres of influence plus the volume between the spheres of influence. The drops have both an axial velocity in the direction of the motion of the entire cluster with respect to a frame of reference located outside of the cluster, and a radial velocity with respect to the center of the cluster. It is assumed that this radial velocity induces a self-similar radial motion [23] .

While the flame establishes at the cluster periphery, just as in [25] , Fig. 2a, reproduced from [26] shows that for dense clusters of drops only a fraction of fuel has burned at the time when the drops have completely evaporated ; and this fraction decreases as the air/fuel mass ratio, Φ^0 decreases. Figure 2b , also reproduced from [26] , displays the ratio of the fuel mass burned fraction to the fraction of fuel mass that escaped the cluster evaluated at the drop disappearance. These plots show that in the dense regime only a fraction of the evaporated fuel can escape from the cluster before the drops disappear, and that with increasing air/fuel mass ratio this fraction reaches asymptotically unity, in agreement with the classical, isolated drop theory. When Φ^0 is smaller, $(f_B/f_{F1})_{R=0}$ is smaller because more fuel is ejected from the cluster, making the flame stronger and increasing its distance from the cluster. This vigorous burning reduces the drop lifetime, leaving a larger amount of fuel vapor to be burned. The same effect explains why the values of $(f_B/f_{F1})_{R=0}$ are smaller for turbulence model 2, which represents a stronger turbulence at the cluster boundary than that of turbulence model 1. The findings of Bellan and Harstad [26] agree with the experimental observations of Koshland [27] which show that when a collection of drops burns, fuel vapor is still present after the drop have completely evaporated. This general result is independent of the turbulence model used to describe transport at the cluster boundary, as illustrated in Fig.2.

2.2 Electrostatically Charged Clusters of Drops

The difference in the parameters controlling the dynamics of dense and dilute clusters of drops is also evident in Fig.3 reproduced from Harstad and Bellan [23] where the dispersion of electrostatically charged drops is studied. It is seen that electrostatic charging has no effect on the evaporation time of dilute clusters of drops whereas it considerably reduces the lifetime of drops in dense clusters. The charge ratio is calculated with respect to the maximum charge that a drop may sustain before Rayleigh instability occurs ; this charge was shown by Kelly [28] to be $(q_d)_{\max} = (7.34 \times 10^{-11} \text{ coul cm}^{-1}) R^0$, where R^0 is the drop initial radius. In the dilute regime, the drops are too far apart for the electrostatic charge to make an impact on the drop motion, and thus there is no change in the evaporation time. In contrast, the electrostatic force affects the motion of the drops contributing a source term proportional to the drop number density in the radial slip and gas energy conservation equations. Since the drop velocity is a solution of the radial slip conservation equation, and since the evaporation rate is enhanced both by the increased velocity and by

the increased radius of the sphere of influence as the drops repel each other, the evaporation time decreases dramatically. For a charge ratio of unity, the decrease in the evaporation time in the very dense spray regime, beyond that of the asymptotic value obtained in the very dilute regime, may be only an artifact since the exact value of the maximum charge, as defined above, has been experimentally derived and has no theoretical basis.

3 Clusters of Monodisperse Multi-component Drops in Axial Flows

Studies of isolated drops of multi-component fuels in convective flows [29], [30], have revealed that liquid mass diffusion plays an important role in the evaporation of the volatile from the drop. The mechanism through which this occurs is the formation of a circulatory motion inside the drop (in the form of Hill vortices) resulting from the shear induced by the slip velocity at the drop surface. It is this circulatory motion which reduces the large characteristic time (with respect to the drop lifetime) associated with liquid mass diffusion, so that this time becomes shorter than the drop lifetime, and thus contributes to the interplay of phenomena deciding the fate of the volatile.

The results of Harstad and Bellan [24] show that whereas liquid mass diffusion is still important for very dilute clusters of drops, when the volatility of the solute is much larger than that of the solvent (for all practical purposes it is infinite with respect to that of the solvent), liquid mass diffusion is not an important phenomenon for dense or very dense clusters of drops. This is because dense clusters of drops cannot sustain slip velocities with respect to the gas due to the large surface area that they expose to the flow (since the drop number density is large). The large drag force reduces the slip velocity in a time scale that is much smaller than the drop lifetime, and thus shear cannot establish at the drop surface. In absence of shear, there is no circulatory motion inside the drop and the time scale of liquid mass diffusion is again large with respect to the drop lifetime. In this situation, it is no longer mass diffusion which controls evaporation of the volatile, and instead it is surface layer stripping which determines the volatile evaporation rate ; in fact, the volatile evaporates at the same rate as the solvent.

The model yielding these results is based upon the definition of a characteristic number, $Be \equiv -[R/(D_m u_l)]^{0.5}(dR/dt)$, where u_l is the velocity of the vortex motion inside the drop, R is the drop radius, and D_m is the coefficient of mass diffusion in the liquid. When $Be \ll 1$, diffusion into the boundary layer governs the rate of species transfer from the liquid core to the drop surface with subsequent transfer from the drop surface occurring through evaporation. The overall rate of volatile evaporation is governed by the lower of the diffusion rate and the evaporation rate because these are sequential processes. When $Be \gg 1$, volatile transfer from the liquid core to

the boundary layer is no longer controlled by diffusion into the boundary layer, but instead by surface layer stripping. In this case, transfer of volatile from the drop core to the gas is controlled by the higher rate between the diffusion rate and drop regression rate because these are competitive process.

Figure 4, reproduced from [24] , shows precisely this behavior with Be rapidly increasing to very large values for small air/fuel mass ratios and being $O(1) - O(10)$ for moderate to large air/fuel mass ratios. The first situation corresponds to dense clusters of drops whereas the second situation corresponds to dilute clusters of drops. Consistently, Fig. 5, reproduced from the same reference, shows that the mass fraction of the volatile remains frozen inside the drop when the initial drop (and slip velocity, since the gas is initially at rest) is small, corresponding to typical velocities sustained by clusters of drops. When this slip velocity is increased to a value much larger than that sustained by clusters of drops, being however more representative of slip velocities sustained by isolated drops, Fig.6 shows that the volatile profile is no longer frozen in the dilute regime, and thus that liquid mass diffusion starts playing a role. Even with this unrealistically large initial slip velocity, the volatile liquid mass fraction stays frozen practically during the entire drop lifetime ; the initial decrease corresponds to the time taken by the slip velocity to relax. The rapid relaxation of the slip velocity for dense clusters of drops is illustrated in Fig. 7 for initial slip velocities representative of clusters.

4 Clusters of Drops in Vertical Flows

Vortical flows are of general practical interest for drop-laden flows. This configuration also represents the typical turbulent element in any realistic flow, and thus it is of academic interest as well.

4.1 Monodisperse Clusters of Evaporating Drops in Vortical Flows

The model of Bellan and Harstad [31] addresses the dynamics and evaporation of clusters of monodisperse, uniformly distributed drops embedded into large, coherent vortices such' as those encountered in the shear layer of a spray. The vortex is assumed to be cylindrical and infinite, and uniformity is assumed in the axial direction. The model uses the concept of the sphere of influence as described above, but the drop motion is no longer assumed to be self-similar as in the axial flow studies. Drops and gas move in general at different velocities which are the solutions of the radial and azimuthal momentum equations. These equations are solved by assuming that each velocity component can be decomposed into an irrotational motion ($A_{gr}, A_{g\theta}, A_{dr}, A_{d\theta}$, where the subscript g is for gas, r is for radial direction, d is for drop, and θ is for azimuthal direction) and a solid body rotation ($B_{gr}, B_{g\theta}, B_{dr}, B_{d\theta}$).

The centrifugal motion of the gas and drops results in the formation of a cylindrical drop shell representing the cluster volume. The inner vortex core is thus devoid of drops and contains only the initial gas and the fuel vapor left behind by the expanding cluster. The details of the model are presented in [31] .

Figure 8, reproduced from [31], displays the evaporation time, the ratio of the final cluster volume to the initial cluster volume, and the shell thickness ratio as well as the shell thickness. Calculations performed with null or small initial drop solid body rotation could not be continued farther into the dense regime (see Fig.8) because saturation was obtained before complete evaporation. This was an initial indication of the importance of $B_{d\theta}^0$ in the dense regime. In the dilute regime, it turns out that $B_{g\theta}^0$ is more important than $B_{d\theta}^0$ in determining the evaporation time. The cluster volume increase with decreasing air/fuel mass ratio because the larger liquid mass increases the centrifugal force yielding more expansion. The solid body rotation has a major impact on cluster expansion ; as seen in Fig.8, when there is no solid body rotation there is no expansion in the dilute regime and the small expansion in the dense regime is due to the irrotational motion. The irrotational motion and the solid body rotation have opposite effects on the drops because the irrotational motion tends to pack the drops whereas the solid body rotation tends to pull the cluster apart. Thus, when there is no solid body rotation, the shell thickness ratio stays smaller than unit y for all air/fuel mass ratios. The largest cluster expansions and the largest shell thickness ratios are obtained with the largest $B_{d\theta}^0$. The decrease in the shell thickness ratio with increasing air/fuel mass ratio is attributed to the fact that $A_{g\theta}^0 > A_{d\theta}^0$ and thus irrotational motion is transferred from the gas to the drops ; for increasing Φ^0 , the same momentum is transferred to less mass resulting in a larger increase of $A_{d\theta}$ versus the residual drop radius. Therefore, the drops are centrifuged with more packing and the shell stays thinner.

The above discussion also explains why it is also found that the centrifugation of drops in small clusters is characterized by drop packing and shell-thinning, whereas centrifugation of drops in large clusters is characterized by drop dispersion and shell-thickening : in the first case most of the drops reside in the part of the cluster controlled by the irrotational motion, whereas in the second case most of the drops reside in the part of the cluster controlled by the solid body rotation.

Figure 9, also reproduced from [31] shows the correlation between the volume ratio and the shell thickness ratio with St which was here based upon the average azimuthal drop velocity and upon the cluster radius. Since the drop stay confined inside the vortex, results were obtained only for $St \leq 0(1)$. Consistent with the results of Crowe and his coworkers [13] , [14] , the interaction between drops and gas can be entirely quantified in terms of St . The results of Fig.9 show that this is true even for dense clusters of drops, and even when these drops evaporate. As an indication, the evaporation time is also displayed in Fig.9, and, as expected, it does not correlate with St .

4.2 Monodisperse Clusters of Burning Drops in Vertical Flows

The model of Bellan and Harstad [31], has further been used by Fichot et al. [32] to study the unsteady combustion of a cluster of drops inside a vortex.

Similar to the quasi-steady study for drops in axial flows, it was found that the fraction of fuel burned decreases with decreasing air/fuel mass ratio, as shown in Fig.10a. Figure 10b illustrates the fraction of fuel burnt for different $B_{d\theta}^0$. The fact that the variation of the fuel burned fraction is not monotonic with $B_{d\theta}^0$ is evidence of the complex interaction between the drops' dynamics and the flame. When the initial drop tangential velocity is larger, the incipient flame is closer to the cluster. However, the larger centrifugal motion brings the drops closer to the flame, and produces a heat sink at that location. As a result, ignition might be delayed, as shown in Fichot et al.[32]. After an initial transient, this cooling effect is overcome, and the substantial amount of fuel vapor that has accumulated and mixed with oxidizer near the cluster initiates a premixed flame. Thus, initially the flame has a bimodal (premixed and diffusion) character, as shown by plots of the reaction rate versus position presented in Fichot et al. [32]. Initially, the fraction of fuel burned increases with $B_{d\theta}^0$ because the shorter distance between the flame and the cluster results in an increased diffusion flux of fuel to the region outside the cluster. In time, the larger outward drop velocity allows less fuel to escape from the cluster, and the drops become again closer to the flame, thus creating a heat sink. These effects are alternatively present during the combustion process, and there is a critical value of $B_{d\theta}^0$ for which the initial ignition delay is too long to enable a significant amount of fuel to be burned by the time the drops have evaporated (see Fig.10b). Similarly, there is an optimal value of $B_{d\theta}^0$ for which the fraction of burned fuel is maximum, as seen in Fig.10b where this value is 400 s^{-1} for the conditions of the calculation.

5 Summary and Conclusions

The results presented here illustrate the importance of including the coupling between dynamics and thermodynamics when studying the behavior of evaporating or burning clusters of interacting drops. The same conclusion is expected to hold when any heat and/or mass transfer occurs between the two phases.

In the context of drop interactions, this coupling is responsible for a cluster of drops not acting as a single, isolated drop of same size as the cluster, and for qualitatively different phenomena controlling the evaporation of the volatile and solvent for binary-fuel drops in dense and dilute clusters. For clusters of drops embedded in vortices, it is found that the evaporation time is controlled by different characteristics of the motion when the drops belong to dense or dilute clusters. Flames around clusters of drops, such as have been observed experimentally, are found to have a burning efficiency depending strongly of the dynamics of the drops in a cluster which is strongly coupled to the drop number density.

The challenge for future work is to be able to embed submodels, such as those discussed above, into practical spray calculations

ACKNOWLEDGEMENT

This work is provided through the courtesy of the Jet Propulsion Laboratory, California Institute of Technology.

References

- [1] Mao, C-P., Oechsle, V. and Chigier, N. A., "Drop size distribution and air velocity measurements in air assist swirl atomizer sprays", paper 7-6A presented at the CSS/WSS/The Combustion Institute Technical Meeting, San Antonio, Texas, 1985
- [2] Allen, M. G. and Hanson, R. K., "Digital imaging of species concentration field in spray flames", 21st. Symp.(Int.) on Combustion, 1755-1762, 1986
- [3] McDonnell, V. G., Adachi, M. and Samuelsen, G. S., "Structure of reacting and non-reacting swirling air-assisted sprays", Combust. Sci. and Techn., 82, 225-248, 1992
- [4] McDonnell, V. G., Adachi, M. and Samuelsen, G. S., "Structure of reacting and nonreacting, nonswirling, air-assisted sprays, Part II : Drop behavior", Atomization and Sprays, 3,4,411-436, 1993
- [5] Mizutani, Y., Nakabe, K., Fuchihata, M., Akamatsu, F., Zaizen, M. and El-Emarn, S. H., "Spark-ignited spherical flames propagating in a suspended droplet cloud", Atomization and Sprays, 3, 2, 125-135, 1993
- [6] Rudoff, R. C., Brena de la Rosa, A., Sankar, S. V. and Bachalo, W. D., "Time analysis of polydisperse sprays in complex turbulent environments", AIAA-89-0052, Aerospace Sciences Meeting, Reno, Nevada, 1989
- [7] Longmire, E. K. and Eaton, J. K., "Structure of a particle-laden round jet", J. Fluid Mech., 236, 217-257, 1992
- [8] Lazaro, B. J. and Lasheras, J. C., "Droplet dispersion and transport mechanism in a turbulent, free shear-layer", 22nd Symp.(Int.) on Combustion, 1991-1998, 1988
- [9] Lazaro, B. J. and Lasheras, J. C., "Particle dispersion in a turbulent, plane, free shear layer", Phys. Fluids, 1, 6, 1035-1044, 1989
- [10] Hardalupas, Y., Taylor, A. M. K. P. and Whitelaw, J. H., "Particle dispersion in a vertical round sudden-expansion flow", Phil. Trans. R. Sot. Lend., A341, 411-442, 1992

- [11] Elghobashi, S. and Truesdell, G. C., "Direct simulation of particle dispersion in a decaying isotropic turbulence", J. Fluid Mech., 242, 655-700, 1992
- [12] Elghobashi, S. and Truesdell, G. C., "On the two-way interaction between homogeneous turbulence and dispersed solid particles; Part I : turbulence modification", Phys. Fluids A, 5(7), 1790-1801, 1993
- [13] Crowe, C. T., Chung, J. N. and Troutt, T. R., "Particle dispersion by organized turbulent structures", Particulate Two-Phase Flow, Roco, M. C. (Ed.), Butterworth-Heinemann, 626-669, 1993
- [14] Crowe, C. T., Chung, J. N. and Troutt, T. R., "Particle mixing in free shear flows", Prog. Energy Combust. Sci., 14, 171-194, 1988
- [15] Chung, J. N. and Troutt, T. R., "Simulation of particle dispersion in an axisymmetric jet", J. Fluid Mech., 186, 199-222, 1988
- [16] Goix, P., Edwards, C. E., Cessou, A., Dunskey, C. M. and Stepowsky, D., "Structure of a methanol/air coaxial reacting spray near the stabilization region", Combustion and Flame, 98, 205-220, 1994
- [17] Suzuki, T. and Chiu, H. H., "Multi-droplet combustion of liquid propellants", Proceedings of the 9th International Symposium on Space Technology and Science, 145-154, 1971
- [18] Chiu, H. H. and Liu, T. M., "Group combustion of liquid droplets", Combust. Sci. and Techn., 17, 127-142, 1977
- [19] Bellan, J. and Cuffel, R., "A theory of non-dilute spray evaporation based upon multiple drop interaction", Combustion and Flame, 51, 1, 55-67, 1983
- [20] Bellan, J. and Harstad, K., "The details of the convective evaporation of dense and dilute clusters of drops", Int. J. Heat Mass Transfer, 30, 6, 1083-1093, 1987
- [21] Bellan, J. and Harstad, K., "Ignition of non dilute clusters of drops in convective flows", Combust. Sci. and Techn., 53, 2-3, 75-92, 1987
- [22] Bellan, J. and Harstad, K., "Turbulence effects during evaporation of drops in clusters", Int. J. Heat Mass Transfer, 31, 8, 1655-1668, 1988
- [23] Harstad, K. and Bellan, J., "Electrostatic dispersion of drops in clusters", Combust. Sci. and Techn., 63, 4-6, 169-181, 1989
- [24] Harstad, K. and Bellan, J., "A model of the evaporation of binary-fuel clusters of drops", Atomization and Sprays, 1, 367-388, 1991

- [25] **Yang, M.** and **Sichel, M.**, "Unsteady and quasi-steady vaporization of spherical droplet clouds", **AIAA-900-0360**, presented at the 28th Aerospace Sciences Meeting, **Reno, Nevada, 1990**
- [26] **Bellan, J.** and **Harstad, K.**, "Evaporation, ignition and combustion of nondilute clusters of drops", **Combustion and Flame**, **79**, 272-286, 1990
- [27] **Koshland, C. P.**, "Combustion of monodisperse hydrocarbon fuel droplet clouds", Topical Report T.-248, High Temperature Gasdynamics Laboratory, Stanford University, 1985
- [28] **Kelly, A. J.**, "The electrostatic atomization of hydrocarbons", **J. of the Inst. of Energy**, **312**, 1984
- [29] **Sirignano, W. A.**, "Fluid dynamics of sprays", **J. of Fluid Eng.**, **115**, 345-378, 1992
- [30] **Law, C. K.**, "Recent advances in multicomponent and propellant droplet vaporization and combustion", paper **86-WA/HT-14**, presented at the ASME/WAM, Anaheim, California, 1986
- [31] **Bellan, J.** and **Harstad, K.**, "The dynamics of dense and dilute clusters of drops evaporating in large, coherent vortices", **23rd Symp. (Int.) on Combustion**, 1375-1381, 1990
- [32] **Fichot, F.**, **Bellan, J.** and **Harstad, K.**, "Unsteady evaporation and combustion of a drop cluster inside a vortex", **Combustion and Flame**, **98**, 5-19, 1994

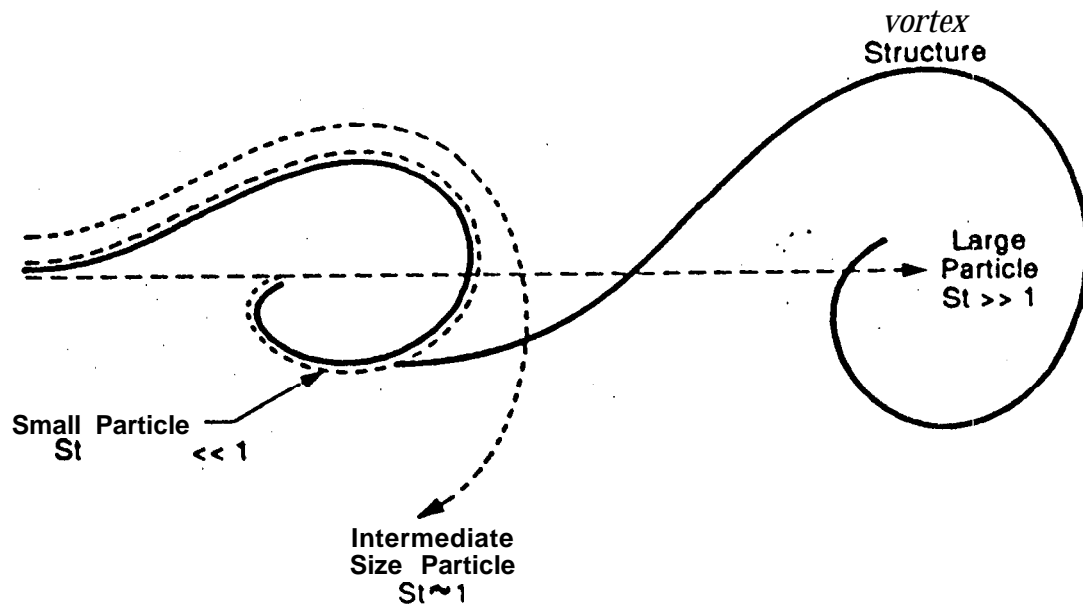


Figure 1. Conceptual model for Stokes number effect on particle spreading in organized structures.

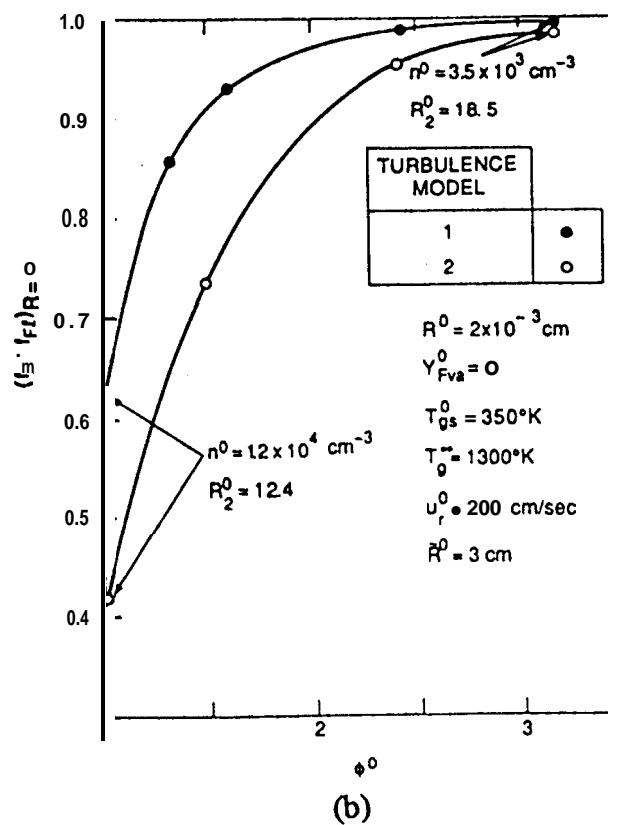
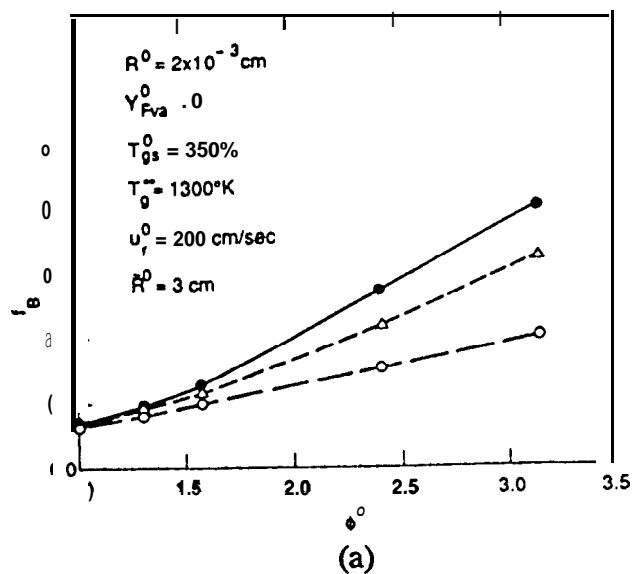


Figure 2. Fuel burned fraction vs initial air-fuel mass ratio. ○, at ignition; ●, at drop disappearance (turbulence Model 1); ▲, at drop disappearance (turbulence Model 2), and (b) ratio of the fuel mass burned fraction to the fraction of fuel mass that escaped the cluster, evaluated at drop disappearance versus ϕ^0 for two models of turbulent transport to the cluster.

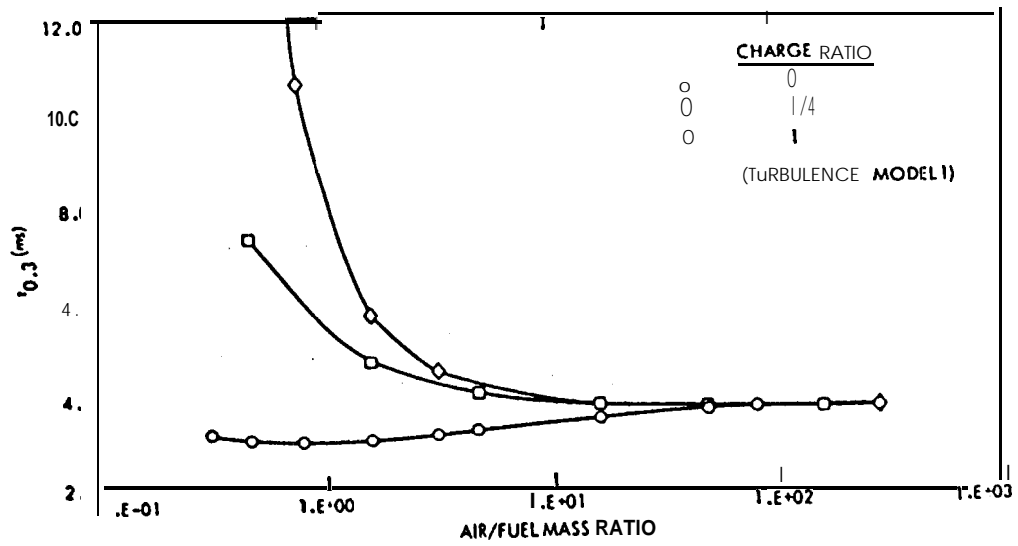


Figure 3. Characteristic evaporation time vs initial air/fuel mass ratio. Drop charge is relative to maximum. See text.

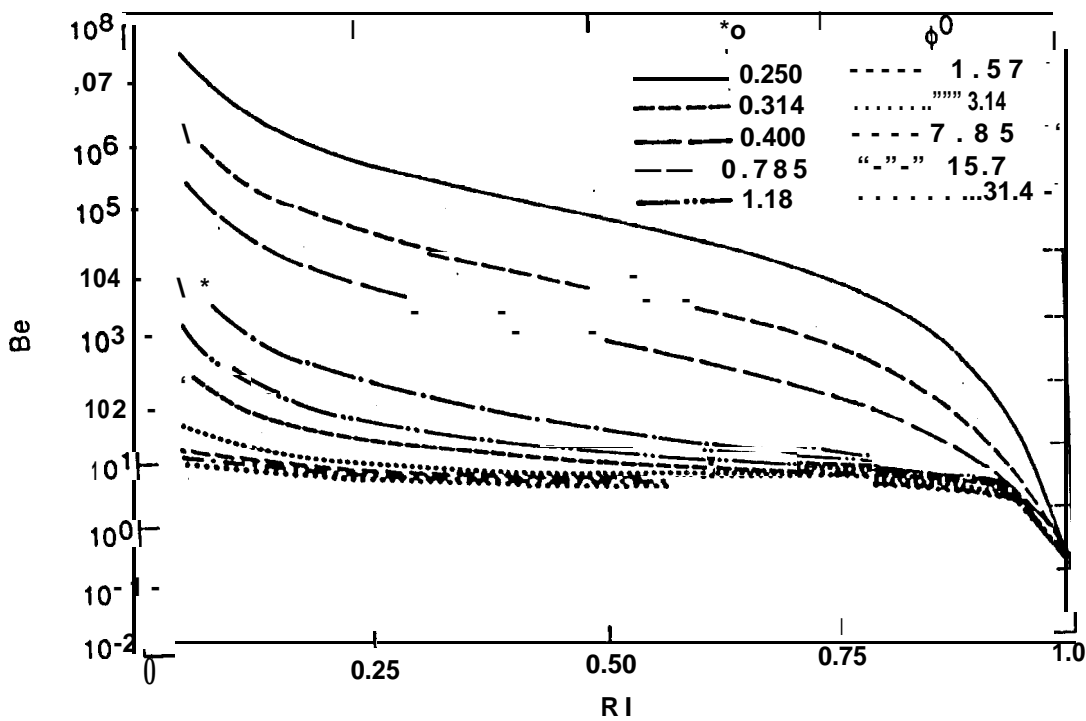


Figure 4. Variation of Be with the residual drop radius for several initial air/fuel mass ratios for a strong turbulence case; $T_{ga}^0 = 1000\text{ K}$, $T_{gs}^0 = 350\text{ K}$, $Y_{HV,c}^0 = 0.02$, $u_d^0 = 200\text{ cm/s}$, $\bar{R}^0 = 3\text{ cm}$, $R^0 = 2 \times 10^{-3}\text{ cm}$, $Y_{Fva}^0 = 0$; No.2-GT/n-decane.

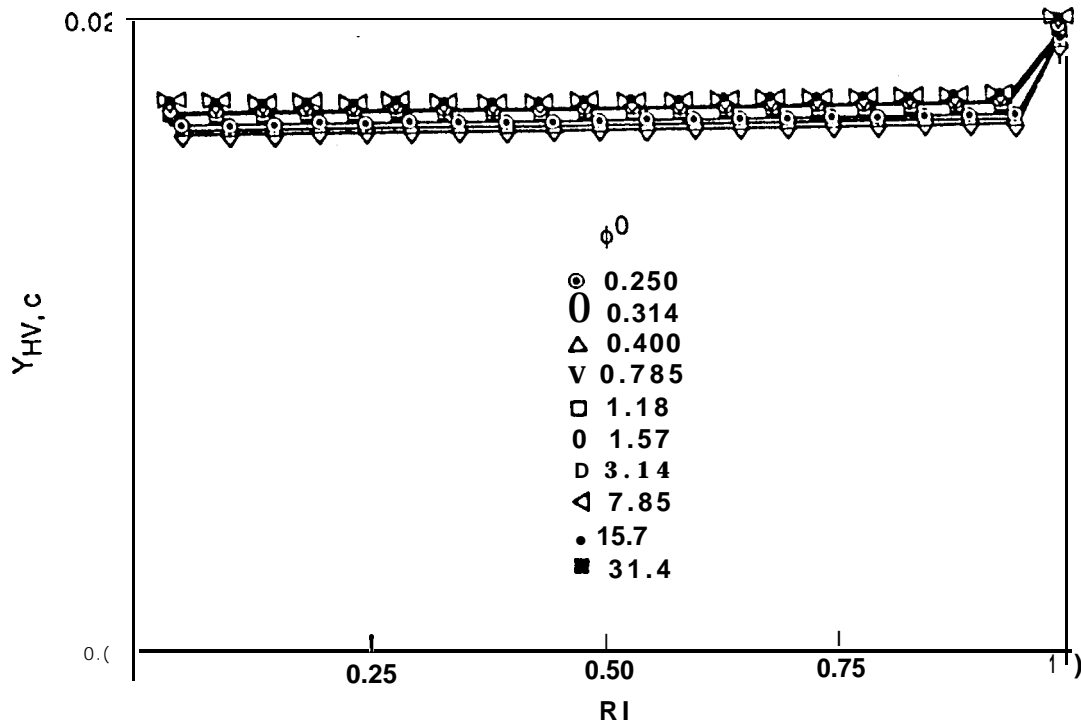


Figure 5. Variation of the liquid mass fraction of the volatile with the residual drop radius for several initial air/fuel mass ratios for a strong turbulence case; $T_{ga}^0 = 1000 K$, $T_{gs}^0 = 350 K$, $Y_{HV,c}^0 = 0.02$, $u_d^0 = 200 cm/s$, $\bar{R}^0 = 3 cm$, $R^0 = 2 \times 10^{-3} cm$, $Y_{Fva}^0 = 0$; No. 2-GT/n-decane.

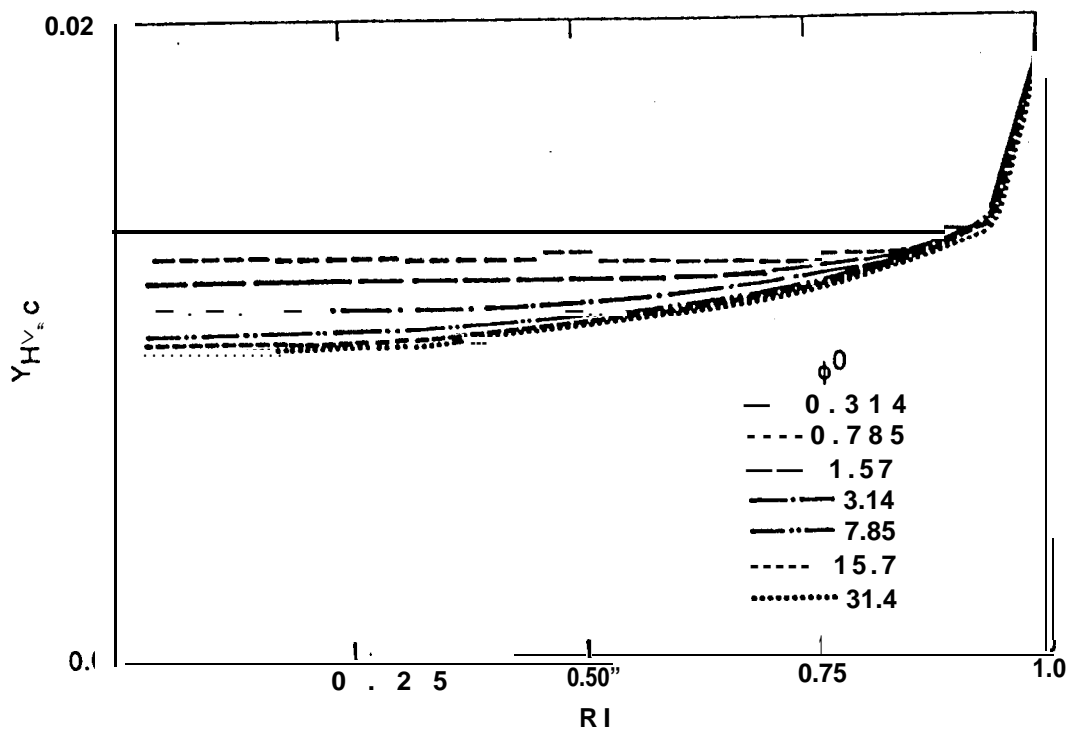


Figure 6. Variation of the liquid mass fraction of the solute with the nondimensional radius of the drop for several initial air/fuel mass ratios for a strong turbulence case; $T_{ga}^0 = 1000 \text{ K}$, $T_{gs}^0 = 350 \text{ K}$, $u_d^0 = 1000 \text{ cm/s}$, $Y_{Fva}^0 = 0$, $Y_{Hv,c}^0 = 0.02$, $\tilde{R}^0 = 3 \text{ cm}$, $R^0 = 2 \times 10^3 \text{ cm}$; No. 2-GT/n-decane.

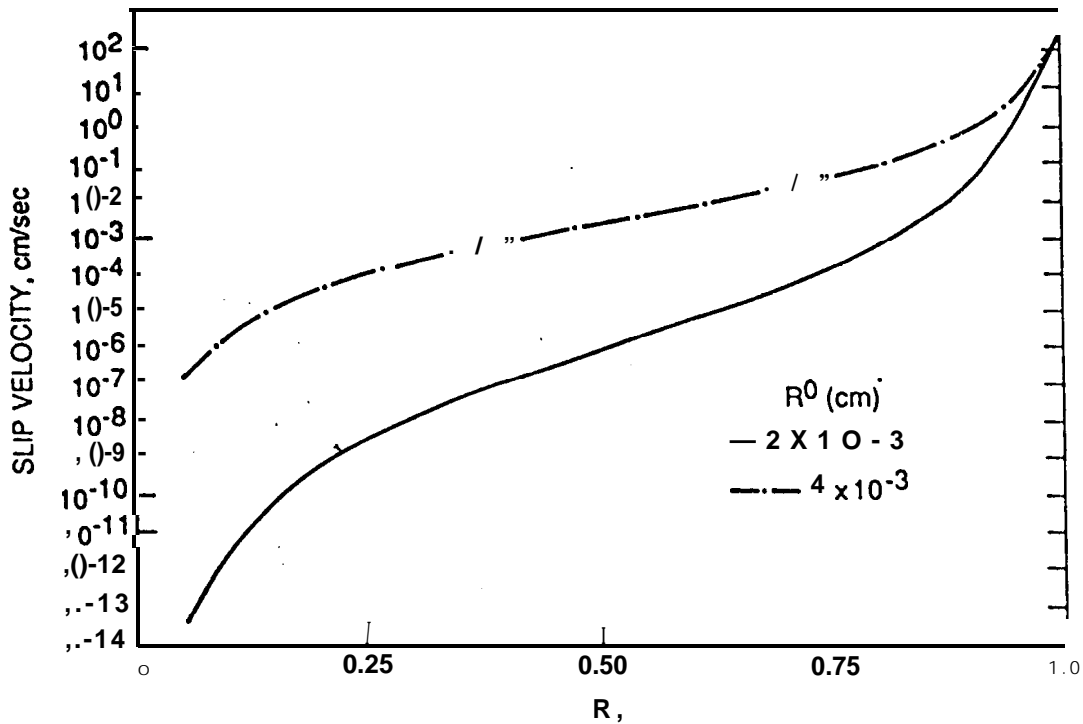


Figure 7.-Decay of the 'slip velocity with the nondimensional drop radius as a function of the initial drop size for a strong turbulence case; for $\phi^0 = 0.314$, $u_d^0 = 200$ cm/s, $T_{ga}^0 = 1000$ K, $T_{gs}^0 = 350$ K, $Y_{Fva}^0 = 0$, $Y_{vc} = 0.02$, $R^0 = 3$ cm; No. 2-GT/n-decane.

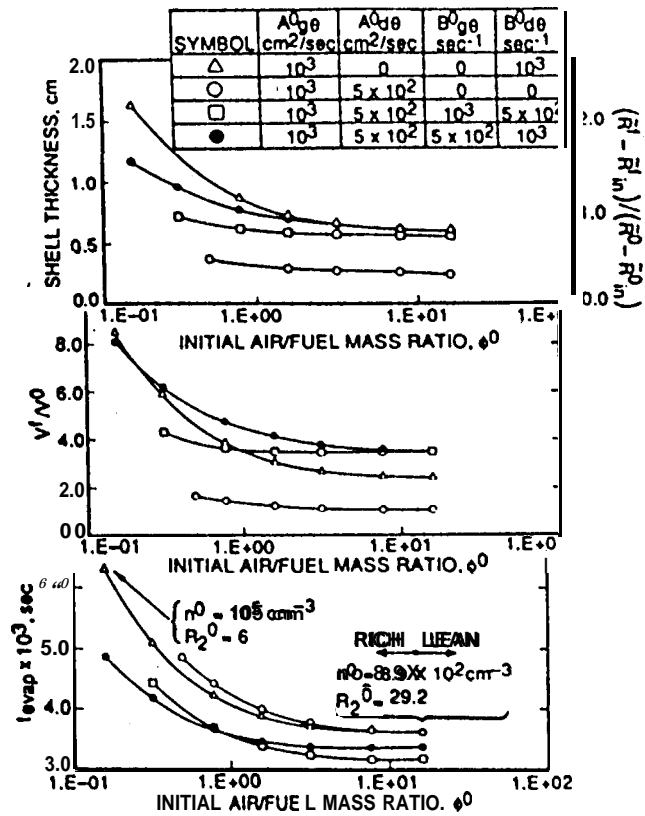


Figure 8. Variation of the evaporation time, volume ratio, final shell thickness and shell thickness ratio versus the initial air/fuel mass ratio. $T_{ga}^0 = 1000 K$, $T_{gs}^0 = 350 K$, $Y_{Fva}^0 = 0$, $R^0 = 2 \times 10^{-3} cm$, $\tilde{R}^0 = 1.0 cm$, $\tilde{R}_{in}^0 = 0.25 cm$, $\rho_l = 0.734 g/cm^3$, $C_p = 0.241 cal/gK$, $C_{pFv} = 0.4 cal/gK$, $L_{bn} = 73.92 cal/g$.

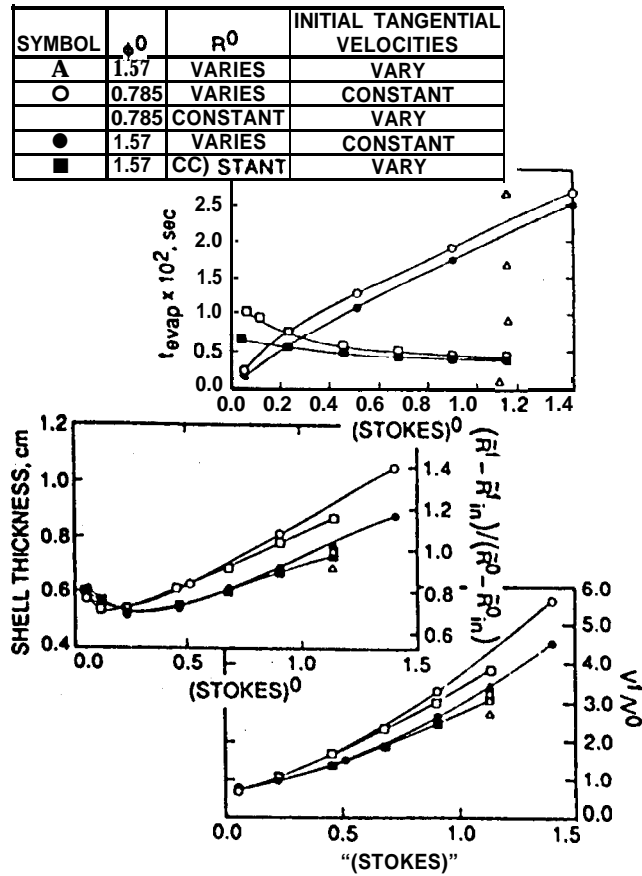
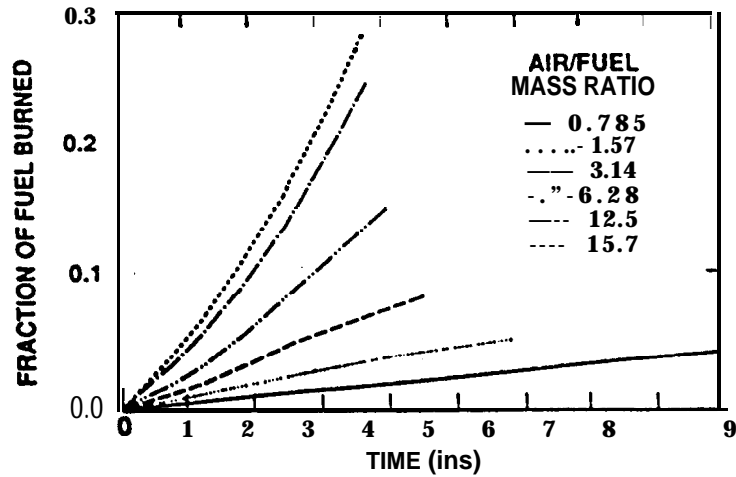
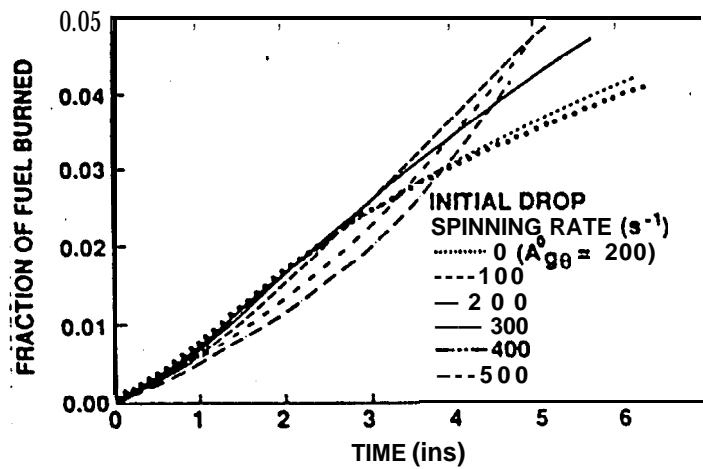


Figure 9. Variation of the evaporation time, volume ratio, final shell thickness and shell ratio with the initial Stokes number for initially dense clusters of drops. $T_{ga}^0 = 1000 K$, $T_w^0 = 350 K$, $Y_{Fva}^0 = 0$, $\tilde{R}^0 = 1.0 cm$, $\tilde{r}^0 = 0.25 cm$, $\tilde{r}_0^0 = 0.25 cm$, $\rho_l = 0.734 g/cm^3$, $C_p = 0.241 cal/gK$, $C_{pFv} = 0.4 cal/gK$, $L_{bn} = 73.92 cal/g$.



(a)



(b)

Figure 10. (a) Fraction of the initial mass of fuel that has burned, as a function of time, for different air/ fuel mass ratios, and (b) fraction of the initial mass of fuel that has burned as a function of time, for different initial drop spinning rates.